

Studies on the Adsorption of Heptamolybdate Ions on AISI 304 Stainless Steel from Acidic HCl Solution for Corrosion Inhibition

Y. Ait Albrimi¹, A. Ait Addi¹, J. Douch¹, M. Hamdani^{1,*}, R.M. Souto²

¹Laboratoire de Chimie Physique, Faculté des Sciences, Université Ibn Zohr, B.P. 8106 Cité Dakhla, Agadir, Morocco.

²Department of Chemistry, University of La Laguna, P.O. Box 456, E-38200 La Laguna (Tenerife, Canary Islands), Spain.

*E-mail: hamdani.mohamed@gmail.com

Received: 17 July 2015 / Accepted: 15 November 2015 / Published: 1 December 2015

Surface interaction of heptamolybdate ions $\text{Mo}_7\text{O}_{24}^{6-}$ on AISI 304 stainless steel (SS) greatly reduces the corrosion rate of the material in acid environments, providing an environmentally-friendly inhibitor system. Corrosion inhibition properties have been studied in naturally aerated 0.5 M HCl solution from weight loss measurements. The influences of inhibitor concentration and solution temperature were investigated. The percentage inhibition efficiency, $S_w(\%)$, increased for increasing concentrations of the ionic inhibitor species. Conversely, the increase of temperature decreased the inhibition efficiency. That is, the corrosion rate, v_{cor} , was faster at higher temperature whereas it was slower for increasing inhibitor concentrations. The adsorption of the inhibitor ions onto the SS surface was found to follow the Langmuir adsorption isotherm. The values of the standard adsorption free energy, ΔG_{ads}^0 , are consistent with a spontaneous physisorption mechanism of the inhibitor ions on the surface of the steel.

Keywords: Stainless steel; Corrosion inhibition; Heptamolybdate ions; Adsorption; Thermodynamic properties; Acidic media.

1. INTRODUCTION

Stainless steel (SS) is the most commonly used material in technological industries such as petroleum extraction and refining, power generation, etc, especially the 300 series AISI stainless steels [1,2]. Among them, type AISI 304 belongs to the group of austenitic stainless steel defined as iron-based alloys, and contains approximately 18.1 wt.% chromium, 8.1 wt.% Ni, and 0.04 wt.% carbon [3]. They can be found in harsh environments containing aggressive chemicals that promote corrosion

reactions [4-7]. Hydrochloric acid is widely used for pickling, descaling, acid cleaning, etc. [8,9]. Generally, in humid environment, stainless steels present a protective film containing chromium oxides/hydroxides that provides good corrosion resistance to the steel surface depending on the nature of both the environment and the metal surface [10]. Yet the presence of chloride ion in the medium is harmful to this passivating film and induces localized attack (e.g., pitting corrosion) which constitutes the principal cause of the failure of these materials [11-14]. The use of inhibitors is one of the best options for the protection of steels against corrosion [15-20]. Since the corrosion rate of metallic materials increases by rising the temperature [21,22], then inhibitor systems should be effective even at elevated temperature [23, 24].

It was found that molybdate ions have remarkable inhibition efficiency for the corrosion protection of steels in acidic media [25-29]. Molybdates are cheap, non-toxic and environmental friendly [30]. The beneficial effect is due to the enrichment of the passive film by molybdates which may retard the growth of pits or crevices on the steel surface [31,32]. It has been reported that the negative ions would predominate in solutions of very low pH, through the distribution diagram of molybdenum species in acidic solutions [33]. The oxyanions as ammonium molybdate and tungstate were used as pitting corrosion inhibitors for 304 SS in deaerated pure water with and without chlorides [16,34,35]. Molybdate and tungstate were also used as corrosion inhibitors for cold rolling steel in hydrochloric acid solution [27].

In a previous report, hexa-ammonium heptamolybdate tetrahydrate was shown to be a promising corrosion inhibitor for 304 SS in 0.5 M HCl at ambient temperature [36]. The aim of this study was to further investigate the inhibition effect of heptamolybdate (HM) ions on 304 stainless steel in hydrochloric acid using weight loss measurements in the temperature range 291 – 313 K. The corrosion rates of the steel in 0.5 M HCl with and without HM were determined, and various parameters describing the kinetics of corrosion of the stainless steel as well as adsorption process of inhibitor were evaluated. The rationale for this investigation was to study the adsorption mode of heptamolybdate ions on the stainless steel surface in order to discriminate whether physisorption or chemisorption account for the interactions. Determination of several parameters related to kinetic activation and the adsorption process may be a tool to ascertain the adsorption mechanism of the inhibitor ion. To this end, correlation between the thermodynamic parameters and the adsorption mechanism was also studied and discussed.

2. EXPERIMENTAL

2.1. Materials and sample preparation

Austenitic AISI 304 SS supplied by Thyssen Krupp Materials International (Mülheim a. d. Ruhr, Germany) were cut into plates of size 1 cm x 1 cm x 0.1 cm. The composition of the stainless steel (in wt. %), determined by Spark Emission Spectrometry, was 18.2 wt.% Cr, 8.02 wt.% Ni, 1.91 wt.% Mn, 0.333 wt.% Si, 0.315 wt.% Mo, 0.304 wt.% Cu, 0.091 wt.% V, 0.057 wt.% N, ≤ 0.052 wt.% C, 0.037 wt.% Nb, 0.032 wt.% P, ≤ 0.01 wt.% S, 0.008 wt.% Ti, Fe in balance. The plates were ground

with emery papers of different grit size, thoroughly washed and ultrasonically cleaned in twice-distilled water and absolute ethanol, for 10 min, and finally dried in air.

All chemicals used in this work, namely hydrochloric acid and hexa-ammonium heptamolybdate tetrahydrate, $(\text{NH}_4)_6\text{Mo}_7\text{O}_{24}\cdot 4\text{H}_2\text{O}$, were reagent grade. 0.5 M hydrochloric acid aqueous solutions were prepared by dilution of the concentrated solution using twice-distilled water. HM was added to the acid solution in concentrations ranging from 10^{-4} to 10^{-3} M. The pH value of the resulting solutions was 0.40 ± 0.02 .

2.2. Weight loss measurements

Plates were immersed, in a hanging position, in 50 ml of 0.5 M HCl solutions both without and containing different concentrations of the inhibitor. The measurements were performed at various temperatures ranging from 291 to 313 K in open air, whereas the data at 298 K were taken from ref. [36]. The samples were weighed before and after immersion, and weight losses were determined using an electronic balance PRECISA 303A (Precisa Gravimetrics AG, Dietikon, Switzerland) with an accuracy of 0.0001 g. The duration of the immersion tests used for the weight loss was 48 hours. The percentage inhibition efficiency, $S_w(\%)$, and the degree of surface coverage, θ , were calculated by means of:

$$S_w(\%) = \frac{W_0 - W}{W_0} \times 100 \quad (1)$$

$$\theta = \frac{S_w}{100} \quad (2)$$

where W_0 and W are the weight losses of 304 SS in the absence and in the presence of the inhibitor, respectively. The weight loss expressed in $(\text{mg cm}^{-2} \text{ day}^{-1})$ stands for the corrosion rate of the steel, v_{cor} .

The naturally-aerated solutions were stagnant, and temperature control was performed using a thermostat-cooling condenser. Each measurement was performed on three separate samples, and average values of weight losses are given. The standard deviation of the observed weight loss was less than 6%.

3. RESULTS AND DISCUSSION

3.1. Effect of concentration

Weight loss measurements were carried out both in 0.5 M HCl base solution, and in the acid solution containing different concentrations of HM. Table 1 summarizes the values of the corrosion rates, v_{cor} , expressed in $(\text{mg cm}^{-2} \text{ day}^{-1})$, the percentage inhibition efficiencies, $S_w(\%)$, and the surface coverages, θ , of 304 SS for different concentrations of the inhibitor that were measured at 291 K. The percentage inhibition efficiency and the surface coverage were calculated using Eq. (1) and (2),

respectively. Inspection of Table 1 shows that the corrosion rate decreased, and inhibitor efficiency increased consequently, with increasing contents of HM in 0.5 M HCl solution. The maximum value of $S_w(\%)$ was 91.2%, and it was observed for the solution containing 10^{-3} M HM at 291 K. Any further increase in concentration did not cause any appreciable change in the performance of the inhibitor. This result leads to the conclusion that HM is a highly efficient inhibitor of 304 SS corrosion in 0.5 M HCl solution. The inhibition behaviour of HM ions against corrosion of SS can be attributed to their adsorption on the steel surface by forming a barrier which prevents aggressive ions to reach the surface of the material. Therefore, the inhibitor is adsorbed at the SS/electrolyte interface, and the adsorbed species physically separates the covered steel surface from the corrosive medium. This inhibitory effect of HM merits to be studied at higher temperatures.

Table 1. Corrosion parameters obtained from weight loss of 304 stainless steel in 0.5 M HCl containing different concentrations of HM at 291 K.

T, K	C, M	$v_{cor},$ $mg\ cm^{-2}\ day^{-1}$	$S_w(\%)$	θ
291	0	8.16	-----	-----
	1×10^{-4}	5.33	34.7	0.34
	2×10^{-4}	3.77	53.8	0.53
	5×10^{-4}	2.04	75.0	0.75
	8×10^{-4}	1.24	85.0	0.85
	1×10^{-3}	0.72	91.2	0.91

3.2. Effect of temperature

The effect of temperature on the inhibition efficiency of SS for various concentrations of inhibitor was also determined in the range of temperatures from 298 to 313 K, and it is summarized in Table 2. It can be observed that the corrosion rates of 304 SS increased with the increasing temperature for every inhibitor concentration while the percentage inhibition efficiencies decreased with increasing the temperature. Thus, for a given inhibitor concentration, the inhibition efficiency decreased with the increase in temperature, as illustrated in the case of 10^{-3} M of HM by a decrease from 91.2% at 291 K to 58.3% at 313 K (cf. Tables 1 and 2, respectively). As the temperature increases, the inhibitor desorbs and the surface becomes less protected. Then the inhibitor loses gradually its effectiveness, a feature supporting the physisorption of the inhibitor ion on the surface of the steel. That is, the increase in temperature destabilizes the adsorbed film, and the equilibrium reaction is shifted towards the desorption process instead of the adsorption process [37]. Yet, it must be considered that the kinetics of steel corrosion is also influenced by the rising temperature.

Table 2. Corrosion parameters obtained from weight loss of 304 stainless steel in 0.5 M HCl containing different concentrations of HM after 48 h exposure in the temperature range from 298 to 313 K. Data at 298 K were taken from ref. [36] for comparison.

T, K	C, M	$v_{cor},$ $mg\ cm^{-2}\ day^{-1}$	$S_w(\%)$	θ
298	0	9.50	-----	-----
	1×10^{-4}	6.07	36.1	0.36
	2×10^{-4}	4.51	52.5	0.52
	5×10^{-4}	2.50	73.7	0.73
	8×10^{-4}	2.01	78.8	0.79
	1×10^{-3}	1.4	85.1	0.85
303	0	14.83	-----	-----
	1×10^{-4}	9.62	35.1	0.35
	2×10^{-4}	6.33	49.4	0.49
	5×10^{-4}	4.20	71.7	0.71
	8×10^{-4}	3.80	74.4	0.74
	1×10^{-3}	2.45	83.5	0.83
308	0	20.42	-----	-----
	1×10^{-4}	13.80	32.4	0.32
	2×10^{-4}	10.92	46.5	0.46
	5×10^{-4}	8.76	57.1	0.57
	8×10^{-4}	7.40	64.4	0.64
	1×10^{-3}	5.40	73.6	0.73
313	0	22.94	-----	-----
	1×10^{-4}	17.48	23.8	0.23
	2×10^{-4}	14.52	36.7	0.36
	5×10^{-4}	13.10	42.9	0.42
	8×10^{-4}	10.66	53.6	0.53
	1×10^{-3}	9.58	58.3	0.58

In order to gain more insights on the corrosion process, the Arrhenius law was used to determine both the activation energy, E_a , and the pre-exponential factor, A . The plots shown in Figure 1 are straight lines with regression coefficients close to unity. The values of the kinetic parameters E_a and A derived from these Arrhenius plots are listed in Table 3. The activation energies, E_a , for the

inhibited solutions were higher than those for the uninhibited solution. This can be attributed to the occurrence of an energy barrier for the corrosion reaction due to the presence of inhibitor ions at the metal/electrolyte interface. The observed variation of E_a values may be explained in terms of a change in the mechanism of the corrosion process in the presence of adsorbed inhibitor onto the steel surface [38]. Both increasing [38,39] and decreasing [40-45] trends for the variation of E_a with the inhibitor concentration have been described in the literature. Decreased activation energy values for corrosion process in the presence of the inhibitor can be associated to its chemisorption, while higher values to its physical adsorption [46]. In this work, both the apparent activation energies, E_a , and the pre-exponential factor A increased with increasing HM concentration. The study showed that the decrease of the v_{cor} by increasing inhibitor concentration and E_a is the main factor. HM succeeded to retard the corrosion of the steel, but its inhibition ability diminished at higher temperature. The increase of the temperature leads to decreasing $S_w(\%)$ and increasing E_a values which is often interpreted as an indication of physical adsorption, whereas the opposite trend is regarded to indicate chemisorption of the inhibitor species on the metal surface [9,47,48]. It was also reported that E_a values of the corrosion process vary in the range of 57.7–87.8 kJ mol⁻¹ in acidic media, while most are grouped around 60.7 kJ mol⁻¹ [48], which is in the same order of magnitude of E_a values found in the present work.

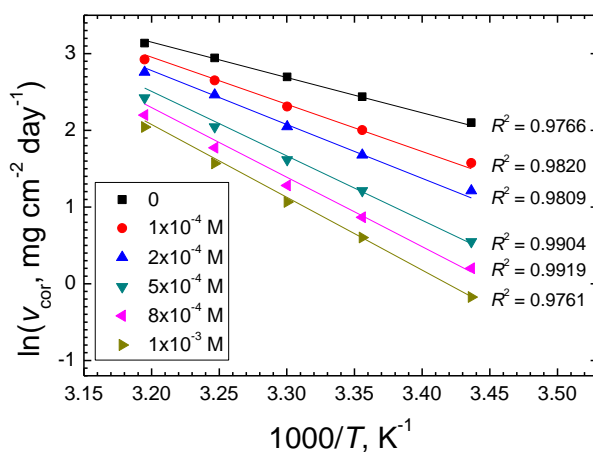


Figure 1. The effect of temperature on the corrosion rate of 304 stainless steel in 0.5 M HCl containing different concentrations of HM.

An alternative form of Arrhenius equation is the transition state equation, Eq. (3), that allows the determination of the enthalpy of activation, ΔH_a^0 , and of the entropy of activation, ΔS_a^0 , for the corrosion process of the stainless steel [49]:

$$v_{cor} = \frac{RT}{hN} \exp\left(\frac{\Delta S_a^0}{R}\right) \exp\left(-\frac{\Delta H_a^0}{RT}\right) \tag{3}$$

Figure 2 depicts straight lines with linear regression coefficients close to 1 when plotting $\ln(v_{cor}/T)$ against $1/T$, supporting that corrosion of 304SS in hydrochloric acid solution can be

elucidated using the kinetic model. $\Delta H_{\alpha}^{\circ}$ and $\Delta S_{\alpha}^{\circ}$ values determined at various temperatures are listed in Table 3. The positive values of the enthalpy changes reflect the endothermic character of the steel dissolution process, suggesting that the dissolution of SS becomes slower in the presence of the inhibitor [9]. On the other hand, the negative values of the entropy change, $\Delta S_{\alpha}^{\circ}$, imply that the formation of the activated complex involved in the rate determining step corresponds to an association instead of a dissociation step. That is, there is a decrease in disorder as the reaction coordinate advances from the reactants to the corresponding activated complex [50].

Table 3. Values of activation parameters for 304 stainless steel in 0.5 M HCl containing different concentrations of HM.

C, M	E_{α} , kJ mol ⁻¹	$10^{-12} \times A$	$\Delta H_{\alpha}^{\circ}$, kJ mol ⁻¹	$(E_{\alpha} - \Delta H_{\alpha}^{\circ})$, kJ mol ⁻¹	$-\Delta S_{\alpha}^{\circ}$, J mol ⁻¹ K ⁻¹	$\Delta G_{\alpha}^{\circ}$, kJ mol ⁻¹				
						291 K	298 K	303 K	308 K	313 K
0	38.27	0.00006	35.76	2.51	134.55	74.91	75.86	76.53	77.20	77.87
1×10^{-4}	51.18	0.0003	48.68	2.51	94.83	76.27	76.94	77.41	77.89	78.36
2×10^{-4}	58.43	0.007	55.92	2.51	73.12	77.20	77.71	78.08	78.44	78.81
5×10^{-4}	69.86	8.2	67.35	2.51	39.63	78.88	79.16	79.36	79.56	79.76
8×10^{-4}	75.34	70	72.84	2.51	23.00	79.53	79.67	79.80	79.92	80.03
1×10^{-3}	78.92	5687	76.42	2.51	13.37	80.31	80.40	80.47	80.54	80.60

Similar observations were reported for the dissolution of mild steel dissolution in HCl solution both in the absence and in the presence of organic inhibitors [51,52]. Conversely, an increase of $\Delta S_{\alpha}^{\circ}$ with increasing inhibitor concentration would reveal that greater disordering occurs on going from the reactant to the activated complex, and it has been reported also for mild steel in acidic environment in the case of other inhibitors [41,53]. Therefore, by considering the behaviour of the kinetic parameters given in Table 3, there is additional evidence for a physical adsorption mechanism to account for the interaction of HM ions with the surface of stainless steel in 0.5 M HCl solution. The validity of this assumption is confirmed by the observation that the values of E_{α} and $\Delta H_{\alpha}^{\circ}$ given in Table 3 evolve in the same extent and verify the relationship $E_{\alpha} - \Delta H_{\alpha}^{\circ} = RT$. Furthermore, these experimental values are very close to the calculated value (2.51 kJ mol⁻¹ at 303 K) evidencing that the corrosion process is a unimolecular reaction.

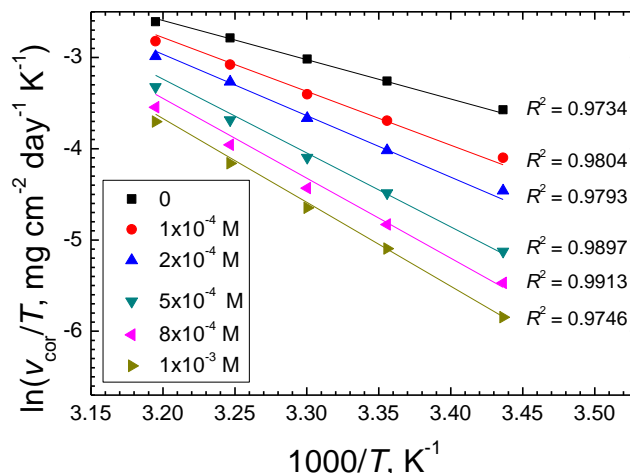


Figure 2. Variation of $\ln v_{cor}/T$ versus $1/T$ plots of 304 stainless steel in 0.5 M HCl containing different concentrations of HM.

The change in free energy of activation ΔG_a^0 for the corrosion process was calculated for each temperature using the ΔH_a^0 and ΔS_a^0 values obtained above. The resulting values of ΔG_a^0 are positive and increased with increasing concentration and temperature. This observation evidences that the activated complex was not stable analogously to previous observations involving N,N0-[(methylimino)dimethylidyne]di-2,4-xylidine [54] and poly(vinyl alcohol-cysteine) [55].

3.3. Adsorption isotherm

In the case of moderate corrosion rates, and considering quasi-equilibrium adsorption, adsorption isotherms can provide valuable information on the interaction of the inhibitor ions with the metal surface. Accordingly, the values of θ computed using Eq. (2), were fitted to Langmuir, Frumkin and Temkin isotherms. The Langmuir isotherm led to the best fit based on the values of the correlation coefficient R^2 in each case. It is regarded in the Langmuir isotherm that all adsorption sites are independent and equivalent, the former standing for the lack of interaction among neighbouring sites with independence of their occupancy. This isotherm can be expressed as [37]:

$$\frac{C}{\theta} = C + \frac{1}{K_{ads}} \tag{4}$$

where K_{ads} is the equilibrium constant for the adsorption-desorption process, C is the inhibitor concentration, and θ is the surface coverage. Figure 3 shows the linear relationship between C/θ and C with correlation coefficients very close to one. The proposal of a Langmuir-type adsorption for the process is also confirmed by the slope values around one. In addition, the big values of the adsorption equilibrium constant, K_{ads} , given in Table 4 demonstrate the high ability of the inhibitor to adsorb on the surface of stainless steel.

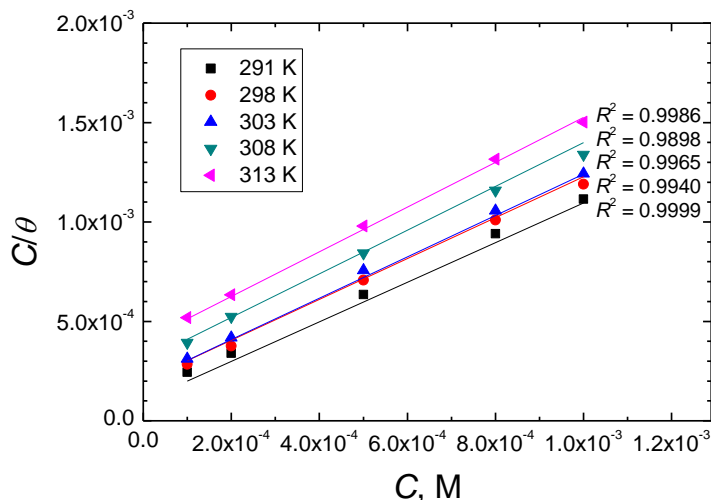


Figure 3. Fits of HM adsorption on 304 stainless steel surface in 0.5 M HCl according to Langmuir model at different temperatures.

Table 4. Thermodynamic parameters of the adsorption of HM on 304 stainless steel as a function of the temperature.

T, K	K_{ads}, M^{-1}	$\Delta G_{ads}^0, kJ mol^{-1}$	$\Delta H_{ads}^0, kJ mol^{-1}$	$-\Delta S_{ads}^0, J mol^{-1} K^{-1}$
291	7043	-31.16	-36.26	17.52
298	5542	-31.31		16.60
303	4845	-31.50		15.70
308	3184	-30.94		17.25
313	2502	-30.81		17.37

On the other hand, ΔG_{ads}^0 can be determined from the K_{ads} value, using 55.5 as the number of moles of water in the solution [56]. This procedure leads to $\Delta G_{ads}^0 = -31.16 kJ mol^{-1}$ at 291 K. It is usually regarded that an absolute value of $|\Delta G_{ads}^0| < 40 kJ mol^{-1}$ stands for a physisorption process [57,58]. Analogously, the adsorption enthalpy, ΔH_{ads}^0 , and the adsorption entropy, ΔS_{ads}^0 , are given by the Van't Hoff equation. That is, the plot of $\ln(K_{ads})$ vs. the reciprocal of temperature must be a straight line of slope $-\Delta H_{ads}^0 / R$, and intercept $[(\Delta S_{ads}^0 / R) - \ln(55.55)]$, respectively [59]. Figure 4 shows the linear dependence of $\ln(K_{ads})$ with $1/T$, from which the adsorption enthalpy, ΔH_{ads}^0 , and the adsorption entropy, ΔS_{ads}^0 , were determined to be $-36.28 kJ mol^{-1}$ and $-16.90 J mol^{-1} K^{-1}$, respectively. The negative value of ΔH_{ads}^0 shows the exothermic character of the adsorption process, that may form

an ordered film at the steel surface. Next, the value of the adsorption enthalpy, ΔH_{ads}^0 , was also estimated using the Gibbs–Helmholtz equation. Figure 5 shows a linear behaviour between $\ln(\Delta G_{ads}^0/T)$ and $1/T$, with slope $\Delta H_{ads}^0 = -36.26 \text{ kJ mol}^{-1}$, which is in good agreement with the value previously obtained using the Van't Hoff equation.

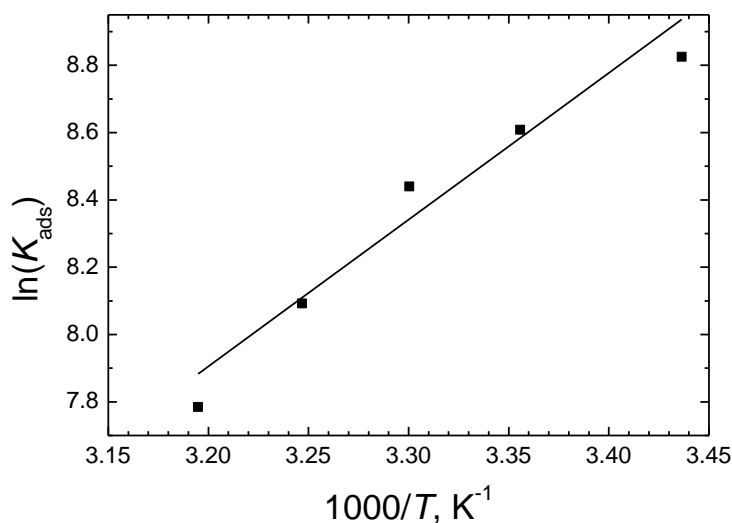


Figure 4. Plot of $\ln K_{ads}$ as a function of the reciprocal temperature for the adsorption of HM ions on 304 stainless steel in 0.5 M HCl.

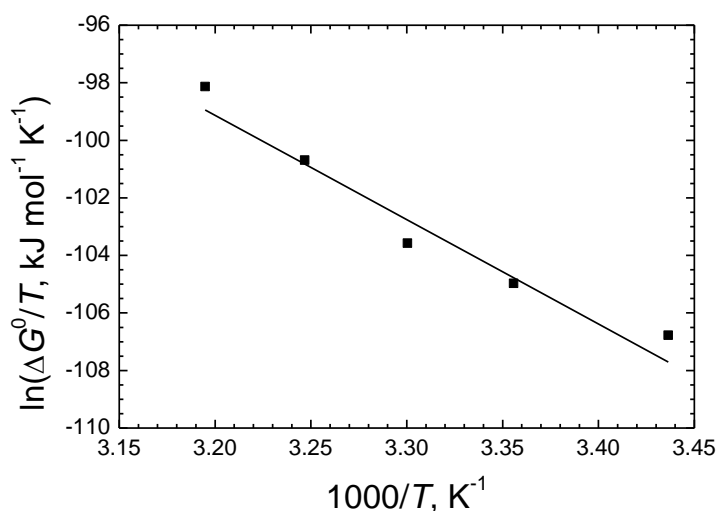


Figure 5. Variation of $\ln(\Delta G_{ads}^0/T)$ with $1/T$ for the adsorption of HM ions on 304 stainless steel in 0.5 M HCl.

The nature of the adsorption mechanism can also be distinguished from the values of the adsorption enthalpy (Durnie 1999), namely $\Delta H_{ads}^0 < 0$ would correspond to physisorption whereas

chemisorption occurs when $\Delta H_{ads}^0 > 0$. Therefore, the data plotted in Figure 5 support a physisorption mechanism to describe the interaction between HM and the SS surface. Finally, the standard adsorption entropy, ΔS_{ads}^0 , may also be deduced using the thermodynamic equation, and the corresponding values are given in Table 4. These values closely match those obtained using the Van't Hoff equation.

4. CONCLUSIONS

Temperature effects on the corrosion inhibition of 304SS by heptamolybdate ions in hydrochloric acid solution were studied in the range of temperatures from 293 to 313 K using the gravimetric method because its easy implementation and its reliability. The inhibition efficiency and thermodynamic parameters of the activation and the adsorption processes were determined.

The weight loss measurements showed that the corrosion rate of steel decreases with increasing the concentration of HM at all tested temperatures. The maximum inhibition efficiency, 91.2%, was observed in presence of 10^{-3} M HM at ambient temperature which qualified this ion to be regarded an efficient inhibitor for 304 SS in 0.5 M HCl. Next, the inhibition efficiencies decreased by rising the temperature.

The values of the apparent activation energy, E_a , obtained for the inhibited solutions were greater than their corresponding values obtained for uninhibited solutions. Indeed, the values of the standard adsorption free energy, ΔG_{ads}^0 , indicate spontaneous adsorption and strong interaction of HM ion onto the surface steel. These values laid barely between the limit values corresponding to physisorption and chemisorption. The negative value of ΔH_{ads}^0 supports that the adsorption of this inhibitor is an exothermic process, though it might involve physisorption, chemisorption, or a mixture of them [50, 60]. But the extent of ΔH_{ads}^0 discriminates between them insofar the value less than -48.86 kJ mol^{-1} is considered to correspond to a physisorption process, while values approaching -100 kJ mol^{-1} are considered for chemisorption [60]. Under such reasoning, the behavior of HM on 304 SS can be acceptably classified as a physisorption process.

The adsorption mode of heptamolybdate ions on the steel surface fits the Langmuir model, and the negative value of ΔG_{ads}^0 is an evidence of their spontaneous adsorption on the metal surface. That is, the negatively-charged HM ion [24] adsorbs onto the positively charged metal surface in competition with the chloride ion following the Langmuir model. Thus, the inhibition efficiency of the heptamolybdate ion against SS corrosion protection is probably due to its ion-molecular structure resulting in localized negative charge densities, which interact with the metal surface. At elevated temperatures, the inhibitor efficiency decreased together with an increase in the activation energy.

ACKNOWLEDGMENTS

Financial support by the CNRST (Rabat, Morocco) through the competence Pôle PECCA, and by the Spanish Ministry of Economy and Competitiveness (MINECO, Madrid, Spain) and the European Regional Development Fund (Brussels, Belgium) under grant CTQ2012-36787, are gratefully acknowledged.

References

1. T.J. Mesquita, E. Chauveau, M. Mantel, N. Bouvier and D. Koschel, *Corros. Sci.*, 81 (2014) 152.
2. M. Finšgar and J. Jackson, *Corros. Sci.*, 86 (2014) 17.
3. *Handbook of Stainless Steel*; Outokumpu Oyj: Espoo (2013), p. 11.
4. R. Nishimura, *Corros. Sci.*, 49 (2007) 81.
5. A. Pardo, M.C. Merino, A.E. Coy, F. Viejo, R. Arrabal and E. Matykina, *Corros. Sci.*, 50 (2008) 780.
6. P.-A. Itty, M. Serdar, C. Meral, D. Parkinson, A.A. MacDowell, D. Bjugović and P.J.M. Monteiro, *Corros. Sci.*, 69 (2013) 149.
7. P.-A. Itty, M. Serdar, C. Meral, D. Parkinson, A.A. MacDowell, D. Bjugović and P.J.M. Monteiro, *Corros. Sci.*, 83 (2014) 409.
8. C.B. Breslin, D.D. Macdonald, E. Sikora and J. Sikora, *Electrochim. Acta*, 42 (1997) 137.
9. I. Ahamad, R. Prasad and M.A. Quraishi, *Corros. Sci.*, 52 (2010) 933.
10. G.T. Burstein, in: *Corrosion. Volume 1: Metal/Environment Reactions*, 3rd edn, L.L. Shreir, R.A. Jarman and G.T. Burstein (Eds.); Butterworth-Heinemann: Oxford (1994), p. 1:118.
11. H.-H. Strehblow, in: *Encyclopedia of Electrochemistry. Volume 4: Corrosion and Oxide Films*, A.J. Bard, M. Stratmann and G.S. Frankel (Eds.); VCH: Weinheim (2003), p. 308.
12. G.T. Burstein, C. Liu, R.M. Souto and S.P. Vines, *Corros. Eng. Sci. Technol.*, 39 (2004) 25.
13. G.S. Frankel and N. Sridhar, *Mater. Today*, 11 (2008) 38.
14. J. Izquierdo, L. Martín-Ruiz, B.M. Fernández-Pérez, L. Fernández-Mérida, J.J. Santana and R.M. Souto, *Electrochim. Acta*, 134 (2014) 167.
15. A.A. Hermas, M.S. Morad and M.H. Wahdan, *J. Appl. Electrochem.*, 34 (2004) 95.
16. C.R. Alentejano and I.V. Aoki, *Electrochim. Acta*, 49 (2004) 2779.
17. W.-C. Chiang, I.-S. Tseng, P. Møller, L.R. Hilbert, T. Tolker-Nielsen and J.-K. Wu, *Mater. Chem. Phys.*, 119 (2010) 123.
18. H. Savaloni and M. Habibi, *Appl. Surf. Sci.*, 258 (2011) 103.
19. A.-R. Grayeli-Korpi and H. Savaloni, *Appl. Surf. Sci.*, 258 (2012) 9982.
20. A.-R. Grayeli-Korpi, H. Savaloni and M. Habibi, *Appl. Surf. Sci.*, 276 (2013) 269.
21. G.T. Burstein, M. Carboneras and B.T. Daymond, *Electrochim. Acta*, 55 (2010) 7860.
22. N. Ebrahimi, M. Momeni, A. Kosari, M. Zakeri and M.H. Moayed, *Corros. Sci.*, 59 (2012) 96.
23. A. Galal, N.F. Atta and M.H.S. Al-Hassan, *Mater. Chem. Phys.*, 89 (2005) 28.
24. F. Eghbali, M.H. Moayeda, A. Davoodi and N. Ebrahimi, *Corros. Sci.*, 53 (2011) 513.
25. G.O. Ilevbare and G.T. Burstein, *Corros. Sci.*, 45 (2003) 1545.
26. S.A.M. Refaey, *Appl. Surf. Sci.*, 240 (2005) 396.
27. G. Mu, X. Li, Q. Qu and J. Zhou, *Corrosion*, 48 (2006) 445.
28. Q. Qu, L. Li, S. Jiang, W. Bai and Z. Ding, *J. Appl. Electrochem.*, 39 (2009) 569.
29. A.S. Alshamsi, *Int. J. Electrochem. Sci.*, 8 (2013) 591.
30. I. Danaee, M.N. Khomami and A.A. Attar, *Mater. Chem. Phys.*, 135 (2012) 658.
31. E. Fujioka, H. Nishihara and K. Aramaki, *Corros. Sci.*, 38 (1996) 1915.
32. P. Jakupi, F. Wang, J.J. Noël and D.W. Shoesmith, *Corros. Sci.*, 53 (2011) 1670.
33. M. Lee, S. Sohn and M. Lee, *Bull. Korean Chem. Soc.*, 32 (2011) 3687.
34. M. Ürgen and A.F. Çakir, *Corros. Sci.*, 32 (1991) 835.
35. P. Selvakumar, B. Balanaga Karthik and C.Thangavelu, *Res. J. Chem. Sci.*, 3 (2013) 87.
36. Y. Ait Albrimi, A. Ait Addi, J. Douch, R.M. Souto and M. Hamdani, *Corros. Sci.*, 90 (2015) 522.

37. D. Wahyuningrum, S. Achmad, Y.M. Syah, B. Buchari, B. Bundjali and B. Ariwahjoedi, *Int. J. Electrochem. Sci.*, 3 (2008) 154.
38. E.A. Noor, *Int. J. Electrochem. Sci.*, 2 (2007) 996.
39. I. El Ouali, B. Hammouti, A. Aouniti, Y. Ramli, M. Azougagh, E.M. Essassi and M. Bouachrine, *J. Mater. Environ. Sci.*, 1 (2010) 1.
40. S. Martinez and I. Stern, *J. Appl. Electrochem.*, 31 (2001) 973.
41. S.S. Abd El-Rehim, M.A.M. Ibrahim and K.F. Khalid, *Mater. Chem. Phys.*, 70 (2001) 268.
42. L. Tang, G. Mu and G. Liu, *Corros. Sci.*, 45 (2003) 2251.
43. X. Li and G. Mu, *Appl. Surf. Sci.*, 252 (2005) 1254.
44. M. Bouklah, B. Hammouti, M. Lagrenée and F. Bentiss, *Corros. Sci.*, 48 (2006) 2831.
45. L. Tang, X. Li, Y. Si, G. Mu and G. Liu, *Mater. Chem. Phys.*, 95 (2006) 29.
46. L. Labrabi, Y. Harek, O. Benali and S. Ghalem, *Prog. Org. Coat.*, 54 (2005) 256.
47. T. Szauer and A. Brandt, *Electrochim. Acta*, 26 (1981) 1219.
48. A. Popova, E. Sokolova, S. Raicheva and M. Christov, *Corros. Sci.*, 45 (2003) 33.
49. F. Bentiss, M. Lebrini and M. Lagrenée, *Corros. Sci.*, 47 (2005) 2915.
50. S. Martinez and I. Stern, *Appl. Surf. Sci.*, 199 (2002) 83.
51. E.A. Noor and A.H. Al-Moubaraki, *Mater. Chem. Phys.*, 110 (2008) 145.
52. B. Zerga, A. Attayibat, M. Sfaira, M. Taleb, B. Hammouti, M. Ebn Touhami, S. Radi and Z. Rais, *J. Appl. Electrochem.*, 40 (2010) 1575.
53. M. Dahmani, A. Et-Touhami, S.S. Al-Deyab, B. Hammouti and A. Bouyanzer, *Int. J. Electrochem. Sci.*, 5 (2010) 1060.
54. A.K. Singh, S.K. Shukla, M.A. Quraishi and E.E. Ebenso, *J. Taiwan Inst. Chem. Eng.*, 43 (2012) 463.
55. A.F.S.A. Rahiman and S. Sethumanickam, *Arab. J. Chem.*, (2014) in press.
<http://dx.doi.org/10.1016/j.arabjc.2014.01.016>.
56. E. Cano, J.L. Polo, A.L.A. Iglesia and J.M. Bastidas, *Adsorption*, 10 (2004) 219.
57. V. Branzoi, F. Branzoi and M. Baibarac, *Mater. Chem. Phys.*, 65 (2000) 288.
58. X. Li, S. Deng and H. Fu, *Corros. Sci.*, 53 (2011) 302.
59. D. Do, *Adsorption Analysis: Equilibria and Kinetics*; Imperial College Press: New York (1998).
60. W. Durnie, R. De Marco, B. Kinsella and A. Jefferson, *J. Electrochem. Soc.*, 146 (1999) 1751.

© 2016 The Authors. Published by ESG (www.electrochemsci.org). This article is an open access article distributed under the terms and conditions of the Creative Commons Attribution license (<http://creativecommons.org/licenses/by/4.0/>).